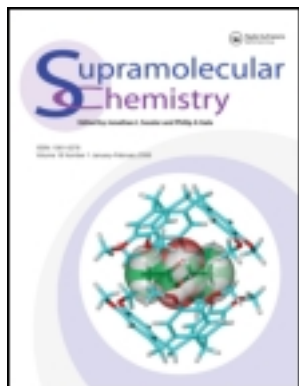


This article was downloaded by: [University of New Hampshire]

On: 19 February 2013, At: 04:10

Publisher: Taylor & Francis

Informa Ltd Registered in England and Wales Registered Number: 1072954 Registered office: Mortimer House, 37-41 Mortimer Street, London W1T 3JH, UK



Supramolecular Chemistry

Publication details, including instructions for authors and subscription information:

<http://www.tandfonline.com/loi/gsch20>

Self-assembling tripeptide as organogelator: the role of aromatic π -stacking interactions in gel formation

Arpita Dutta^a, Dipankar Chattopadhyay^b & Animesh Pramanik^a

^a Department of Chemistry, University of Calcutta, 92, A.P.C. Road, Kolkata, 700009, India

^b Department of Polymer Science and Technology, University of Calcutta, 92, A.P.C. Road, Kolkata, 700009, India

Version of record first published: 18 Jan 2010.

To cite this article: Arpita Dutta, Dipankar Chattopadhyay & Animesh Pramanik (2010): Self-assembling tripeptide as organogelator: the role of aromatic π -stacking interactions in gel formation, *Supramolecular Chemistry*, 22:2, 95-102

To link to this article: <http://dx.doi.org/10.1080/10610270903254142>

PLEASE SCROLL DOWN FOR ARTICLE

Full terms and conditions of use: <http://www.tandfonline.com/page/terms-and-conditions>

This article may be used for research, teaching, and private study purposes. Any substantial or systematic reproduction, redistribution, reselling, loan, sub-licensing, systematic supply, or distribution in any form to anyone is expressly forbidden.

The publisher does not give any warranty express or implied or make any representation that the contents will be complete or accurate or up to date. The accuracy of any instructions, formulae, and drug doses should be independently verified with primary sources. The publisher shall not be liable for any loss, actions, claims, proceedings, demand, or costs or damages whatsoever or howsoever caused arising directly or indirectly in connection with or arising out of the use of this material.

Self-assembling tripeptide as organogelator: the role of aromatic π -stacking interactions in gel formation

Arpita Dutta^a, Dipankar Chattopadhyay^b and Animesh Pramanik^{a*}

^aDepartment of Chemistry, University of Calcutta, 92, A.P.C. Road, Kolkata 700009, India; ^bDepartment of Polymer Science and Technology, University of Calcutta, 92, A.P.C. Road, Kolkata 700009, India

(Received 30 April 2009; final version received 4 August 2009)

While the terminally protected tripeptide Boc-Phe-Gly-*m*-ABA-OMe **I** (*m*-ABA, *meta*-amino benzoic acid) is an excellent gelator of aromatic organic solvents, another similar tripeptide Boc-Leu-Gly-*m*-ABA-OMe **II**, where the Phe residue of peptide **I** is replaced by Leu, cannot form gels with the same solvents. The morphology of the gels of peptide **I**, characterised by the field-emission scanning electron microscopy and high-resolution transmission electron microscopy, reveals the formation of nanofibrous networks which are known to encapsulate solvent molecules to form gels. The wide-angle X-ray scattering studies of the gels suggest the β -sheet-mediated self-assembly of peptide **I** in the formation of a nanofibrous network, where π -stacking interactions of Phe play an important role in the self-assembly and gel formation. The dried gel of peptide **I** observed between crossed polarisers after binding with a physiological dye, Congo red, shows a bluish-green birefringence, a characteristic of amyloid fibrils.

Keywords: peptide; gelator; π -stacking interactions; self-assembly; nanofibrous network

Introduction

Low-molecular-weight organogelators are important due to their potential applications in the field of biomaterials (1, 2), nanotechnology (3, 4), pollution control (5), oil-spill recovery (6), food or cosmetic additives (7), preparing vehicles for drug delivery system (8), light-harvesting materials (9, 10), dental composite carriers (11), in preparing dye-sensitive solar cells (12) and others (13–16). Generally, 3D fibrous networks derived from the self-assembly of low-molecular-mass organic compounds encapsulate bulk solvents under appropriate conditions to form gels. A suitable molecular building block self-assembles through various non-covalent interactions such as hydrogen bonds (17–19), π - π -stacking (20–22), metal coordination (23, 24) and van der Waals interactions (25–27) to form supramolecular gels. Although there are several examples of the formation of organogels through the self-assembly of small organic molecules (28–33), examples of low-molecular-weight acyclic peptide-based organogelators are relatively less (34–39).

It has been observed that π - π interactions play an important role in gel formation (20–22, 34). Therefore, studies are necessary with designed molecules to gain more insights into the influence of π -stacking interactions in gel formation. In this context, we chose two tripeptides Boc-Phe-Gly-*m*-ABA-OMe (**I**) and Boc-Leu-Gly-*m*-ABA-OMe (**II**) (*m*-ABA, *meta*-amino benzoic acid) to study the gel formation (Figure 1). Previously, it has been

observed that dipeptides containing *m*-ABA, a substituted γ -amino butyric acid with an all *trans*-extended configuration, can generate amyloid-like fibrils through β -sheet-mediated self-assembly (40). Therefore, tripeptides **I** and **II** have been designed to incorporate *m*-ABA for creating nanofibrous networks necessary for trapping solvent molecules in gel formation. Since aromatic π - π interactions provide favourable energetic contributions as well as order and directionality in the self-assembly of amyloid structures (41), peptide **I** has been designed to incorporate Phe. In peptide **II**, the Phe residue of peptide **I** has been replaced by Leu to examine the role of π -stacking interactions in the gelation process. The peptides were synthesised using conventional solution-phase methodology. The gels were characterised using field-emission scanning electron microscopy (FE-SEM), high-resolution transmission electron microscopy (HRTEM), wide-angle X-ray scattering (WAXS) studies and Congo red binding assay.

Results and discussion

Gelation property of peptides

In the course of the investigation, it has been observed that peptide **I** can form thermoreversible transparent gels in various organic solvents such as benzene, toluene, *m*-xylene and 1,2-dichlorobenzene (Table 1). The gelating capabilities of the terminally protected tripeptide **I** have been examined in a variety of organic solvents

*Corresponding author. Email: animesh_in2001@yahoo.co.in

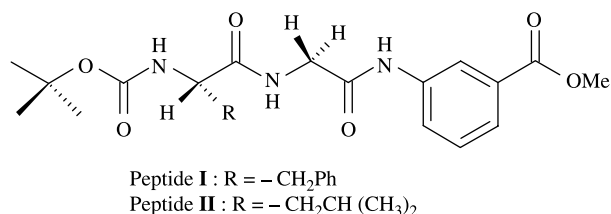


Figure 1. Schematic diagrams of peptides **I** and **II**.

by dissolving a small amount of the compound in 0.5 ml of the solvent under investigation by heating. Upon cooling below the temperature of gelation (T_{gel}), the complete volume of the solvent is immobilised to form gel. The gelation has been confirmed by the inverted test-tube method (Figure 2) (42). Peptide **I** is found to be a quite efficient organogelator to gelify many toxic aromatic solvents at very low concentration ($<2.5\%$, w/v), in certain solvents (Table 1), which is a characteristic feature of a potential gelator. The gels included in Table 1 are stable at room temperature for few weeks and stable towards shaking. The change in sol–gel phase transition temperature with respect to gelation concentration of peptide **I** in toluene is presented in Figure 3, where a steady increase of T_{gel} is observed with the increase in gelation concentration (Table 2). It is noteworthy that only peptide **I** can form gels, but peptide **II**, where the Phe residue of peptide **I** has been replaced by Leu, cannot form gels. Another important feature is that peptide **I** generally forms gels with aromatic solvents. It fails to form gels with non-aromatic solvents such as chloroform, methanol, acetonitrile, acetone and ethylacetate (Table 1). Therefore, it is apparent that the Phe residue of peptide **I** plays an important role in self-association and gelation with aromatic organic solvents.

Proposed model of molecular packing in gel

The self-assembly of peptide **I** is responsible for producing supramolecular gels. Therefore, it is necessary to know the conformation of the peptide which generally controls the

Table 1. Gelation properties of tripeptide **I** in various organic solvents.

Solvent	w/v %	State	Melting point of the gel ($^{\circ}\text{C}$)
Benzene	3.90	Gel	71
Toluene	1.12	Gel	66
<i>m</i> -Xylene	2.40	Gel	68
1,2-Dichlorobenzene	2.10	Gel	68
Chloroform	–	Soluble	–
Methanol	–	Soluble	–
Acetonitrile	–	Soluble	–
Acetone	–	Soluble	–
Ethylacetate	–	Soluble	–

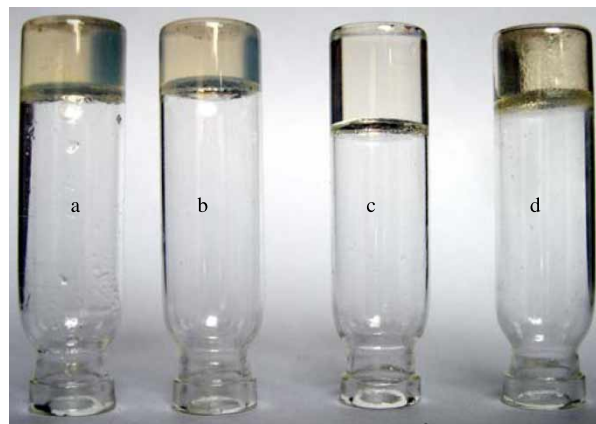


Figure 2. Images of inverted test tubes containing transparent stable tripeptide **I** gels in: (a) benzene; (b) toluene; (c) *m*-xylene and (d) 1,2-dichlorobenzene.

pattern of self-assembly in small peptides. In order to investigate the existence of intramolecular hydrogen bonding and peptide conformation in aromatic organic medium, the solvent dependence of the NH chemical shifts was examined by NMR titrations (43). In this experiment, a solution of peptide **I** in C_6D_6 (3 mM) was gradually titrated against polar $(\text{CD}_3)_2\text{SO}$. The changes in the chemical shifts are presented in Figure 4. The solvent titration shows that by increasing the percentage of $(\text{CD}_3)_2\text{SO}$ in C_6D_6 from 0 to 6.7% (v/v), the net changes in the chemical shift ($\Delta\delta$) values for Phe(1)–NH, Gly(2)–NH and *m*-ABA(3)–NH are 1.7, 2.3 and 1.4 ppm, respectively (Figure 4). The $\Delta\delta$ values demonstrate that all the NH groups of peptide **I** are free and solvent exposed. In a similar experiment with peptide **II**, the net changes in the chemical shift ($\Delta\delta$) values for Leu(1)–NH, Gly(2)–NH and *m*-ABA(3)–NH are found to be 1.8, 2.1 and 1.3 ppm, respectively (Figure 5). Here also, the $\Delta\delta$ values imply that all the three NH groups of **II**

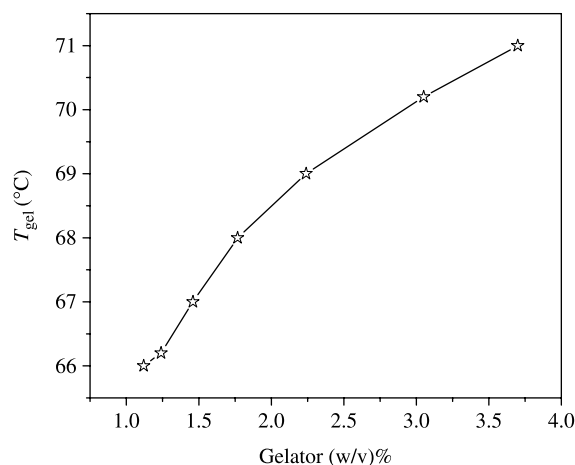


Figure 3. The change in sol–gel phase transition temperature with respect to the gelation concentration of peptide **I** in toluene.

Table 2. The sol–gel phase transition temperature (T_{gel}) of tripeptide **I** in toluene at various gelation concentrations.

Concentration (w/v %)	T_{gel}
3.70	71.0
3.05	70.2
2.24	69.0
1.77	68.0
1.46	67.0
1.24	66.2
1.12	66.0

are solvent exposed. The results show that peptides **I** and **II** do not possess any intramolecular hydrogen bond, indicating an extended conformation in the aromatic solvent C_6D_6 , which is further supported by far-UV circular dichroism (CD) measurement in methanol. The CD pattern of peptides **I** and **II** corresponds to extended structures (Figure 6). Therefore, the results of solvent-dependent NMR titrations and CD measurement favour the conclusion that peptides **I** and **II** mostly remain in extended conformations. Generally, the extended structure of small peptides promotes β -sheet-mediated self-assembly (40).

The WAXS pattern of peptide **I** was measured to obtain the information on the molecular packing in the gel state. The gel of peptide **I** prepared from toluene (4.0% w/v) exhibits a well-resolved X-ray diffraction pattern (Figure 7). A sharp diffraction signal corresponding to a d -spacing of 41.66 Å in the wet gel (Table 3) is approximately close to the length of the molecular duplex of peptide **I**, 39.5 Å, calculated by the INSIGHT II graphic molecular modelling program. In the duplex, two antiparallel molecules of peptide **I** are locked through the intermolecular hydrogen bonds between two m -ABA moieties (Figure 8(a)). Similar d -spacing values, 41.11 Å in the bulk solid and 41.62 Å in the dried gel, indicate the

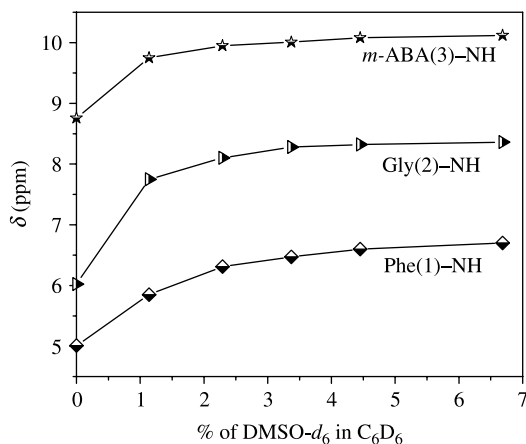


Figure 4. NMR solvent titration curve for NH protons in peptide **I** (initial concentration of **I**, 3 mM in C_6D_6).

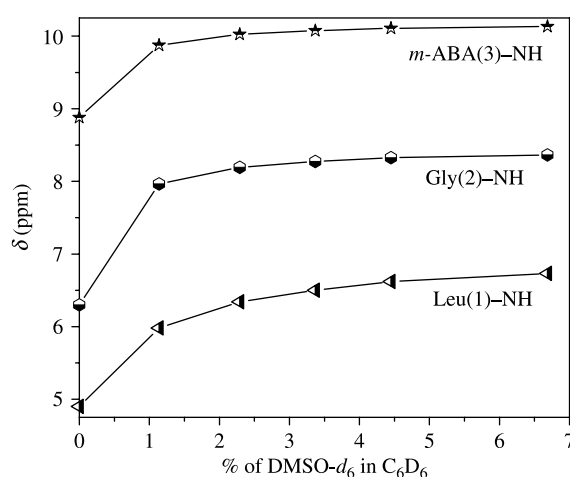


Figure 5. NMR solvent titration curve for NH protons in peptide **II** (initial concentration of **II**, 3 mM in C_6D_6).

presence of the molecular duplex in those states also (Table 3). The duplexes of peptide **I** can stack in the c direction through the intermolecular hydrogen bonds between the peptides' backbones and through the π - π interactions between the phenyl rings of m -ABAs and the phenyl rings of the Phe residues to form β -sheet layers (Figure 8(b)). Several such β -sheet layers of peptide **I** can stack in the a direction to form supramolecular β -sheet structures. The formation of this type of molecular duplex and the packing like 'cross β -model of amyloid fibrils' (44–48) of peptide containing m -ABA have also been reported previously (40). The d -spacings at 5.33, 4.99, 4.07 and 3.26 Å at wide angles ($2\theta < 16^\circ$) in the WAXS pattern are characteristic of the π - π stacking distances between Phe/Phe, Phe/solvent, m -ABA/ m -ABA and m -ABA/solvent, etc. observed in the bulk solid, dried gel and wet gel state of peptide **I** (Figure 7; Table 3). The observed broad peak in the diffraction pattern of the

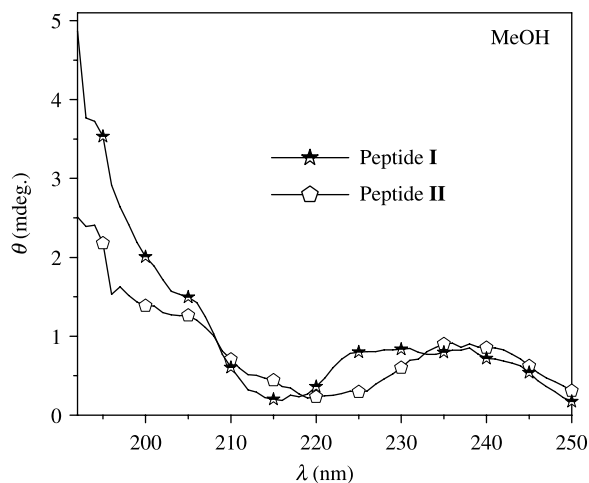


Figure 6. CD curves of peptides **I** and **II**.

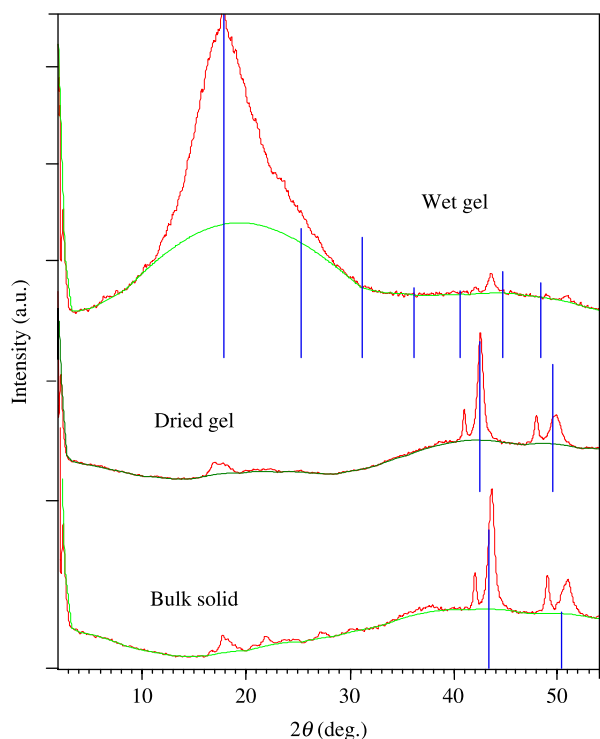


Figure 7. Comparative WAXS patterns of the bulk solid of peptide **I**, dried gel obtained from peptide **I**–toluene (4.0% w/v) and wet gel of peptide **I**–toluene (4.0% w/v).

wet gel is due to heavy scattering from solvent molecules (Figure 7).

The FT-IR spectroscopy is a useful tool to get information about the peptide conformation and intermolecular hydrogen bonding. In the solid state (using the KBr matrix), intense bands have been observed for peptide **I** (dried gel) at 3340 cm^{-1} and for peptide **II** (bulk solid) at 3342 cm^{-1} , which indicates the presence of strongly hydrogen-bonded NH groups (Figure 9). No band has been observed around 3400 cm^{-1} for any of these two peptides in the solid state. The absence of this band suggests that all the NHs for peptides **I** and **II** in the solid state are involved in intermolecular hydrogen bonding. The CO stretching band around $1654\text{--}1695\text{ cm}^{-1}$ (amide **I**) and the NH bending and the C–N stretching peak near 1527 cm^{-1}

Table 3. Major peaks in the WAXS pattern for peptide **I**.

	<i>d</i> -Spacing in Å (position in $^{\circ}2\theta$)
Bulk solid	41.11 (2.15), 35.18 (2.51), 5.33 (16.63), 4.99 (17.75), 4.07 (21.85), 3.26 (27.32), 2.15 (41.99)
Wet gel	41.66 (2.12), 35.19 (2.51), 5.42 (16.33), 4.99 (17.75), 2.08 (43.54)
Dried gel	41.62 (2.12), 35.12 (2.51), 5.11 (17.34), 2.15 (42.00), 2.08 (43.56)

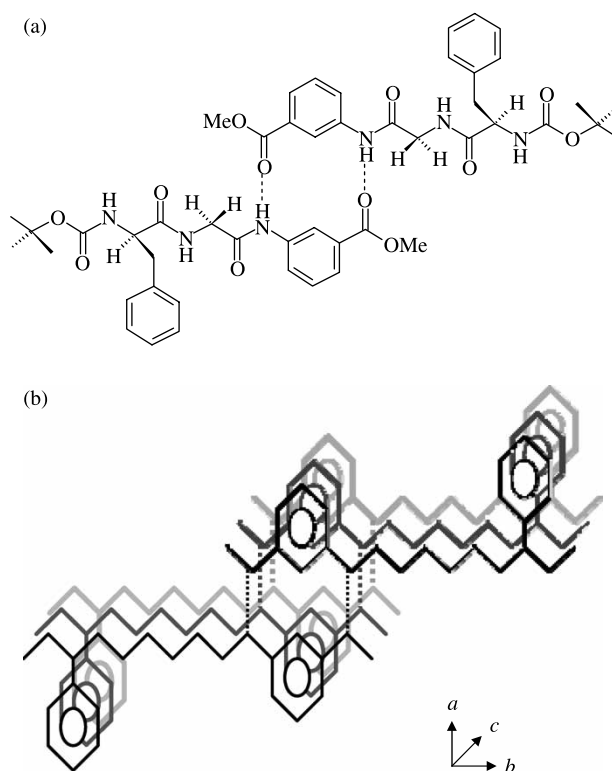


Figure 8. A schematic representation of a tentative model for the molecular packing of the gel phase material of peptide **I**. (a) Showing the formation of a molecular duplex and (b) showing the stacking of the duplexes in the *c* direction to form a β -sheet layer.

(amide **II**) suggest the presence of an intermolecularly hydrogen-bonded β -sheet conformation for peptides **I** and **II** (49).

The regular, parallel alignment of the phenyl rings of Phe in the β -sheet structure of peptide **I** (Figure 8(b)) helps in constructing a nanofibrous network which interacts with the aromatic solvents through π – π interactions to form gels. On the other hand, peptide **II**, where the Phe residue of peptide **I** has been replaced by Leu, cannot form gels due to the lack of π – π interactions.

Morphological studies of gels

The morphology of the assembled peptides **I** and **II** in organic solvents was studied using FE-SEM and HRTEM. The FE-SEM image of the dried gel of peptide **I** obtained from toluene shows the formation of a nanofibrous network (Figure 10(a)). These fibres are found to be 100–120 nm in width and several hundreds of micrometres long (Figure 10(b)). It indicates that peptide **I** possesses the directional forces required for the unidirectional intermolecular interactions between the gelator molecules to form the fibrous nanoscale architecture (50). The HRTEM images of the dried gel of peptide **I** also exhibit a nanofibrous network that can entrap suitable

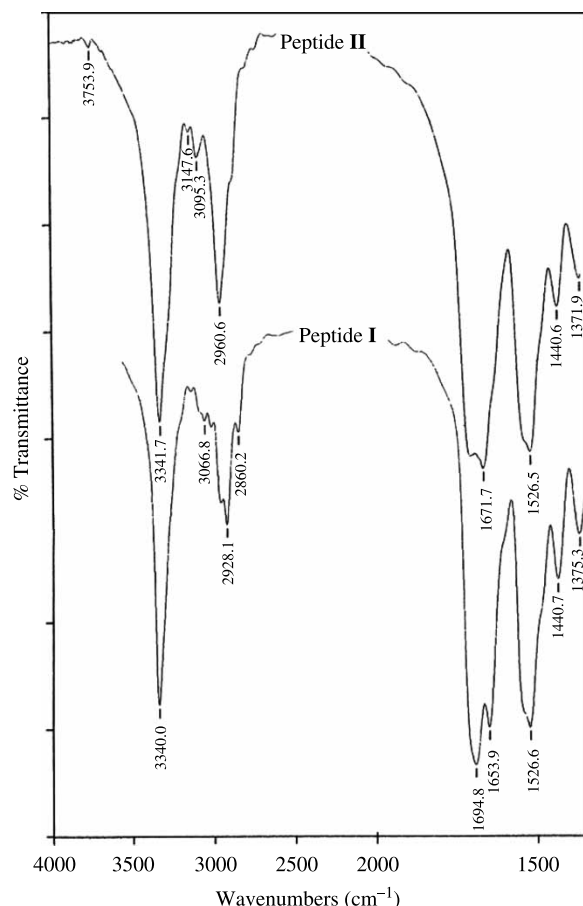


Figure 9. FT-IR spectra at the regions 3200–3500 and 1500–1750 cm^{-1} of peptides **I** (dried gel) and **II** (bulk solid).

solvent molecules effectively (Figure 11(a,b)). The FE-SEM image of peptide **II** obtained from toluene also shows the formation of filamentous fibrillar morphology. These fibres are found to be 400–500 nm in width and several hundreds of micrometres long (Figure 12), therefore they fail to generate a nanofibrous

network which is necessary to form gels. When the stained dried gels of peptide **I** are placed under cross polarisers, the Congo red-bound nanofibrils exhibit a typical bluish-green birefringence, a characteristic of amyloid fibrils (Figure 13) (51). The result supports the proposed model of β -sheet-mediated self-assembly of peptide **I** (Figure 8(b)) in creating a nanofibrous network in the gel state.

Conclusions

This study shows that tripeptide **I**, where the backbone is modified by the extended structure of *m*-ABA, forms molecular duplexes, which on stacking through intermolecular hydrogen bonds and π – π interactions create layers of β -sheets. The layers upon further aggregation generate a nanofibrous network which encapsulates a variety of aromatic organic solvents at very low concentration to form thermoreversible transparent organogels. On the other hand, another similar tripeptide **II**, where the Phe residue of peptide **I** is replaced by Leu, cannot entrap organic solvents. Although peptide **II** generates filamentous fibrils through β -sheet-mediated self-assembly, the non-aromatic Leu residue cannot provide favourable energy, order and directionality in the self-assembly to form a nanofibrous network which is necessary to entrap solvent molecules. From this observation, it is evident that the Phe residue is crucial for the self-assembly and gelation. The present study also shows that even small peptides containing only one Phe can form gels if the backbone of the peptide is suitably modified for β -sheet formation. This observation holds future promise to design and construct low-molecular-weight gelators.

Experimental

Synthesis of peptides

Peptides **I** and **II** were synthesised by conventional solution-phase methods (52). The Boc group was used for

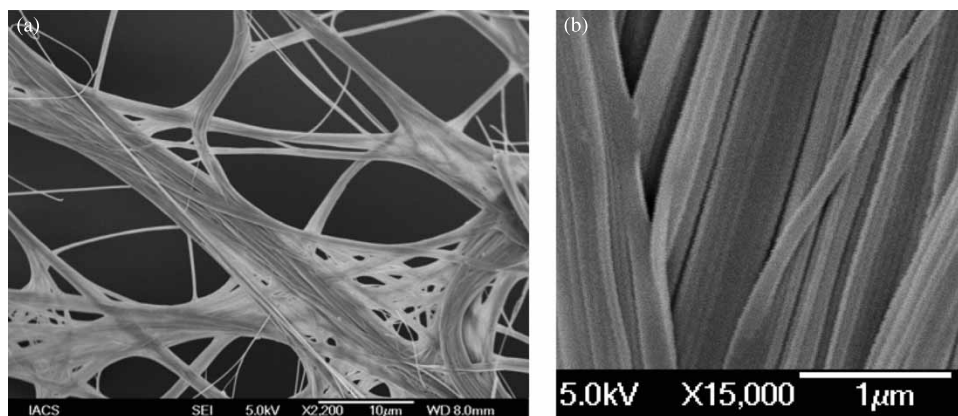


Figure 10. (a) FE-SEM image of the dried gel derived from peptide **I** in toluene showing a nanofibrous network; (b) the enlarged image of the fibrils of the dried gel of peptide **I** with an average diameter of 100–120 nm.

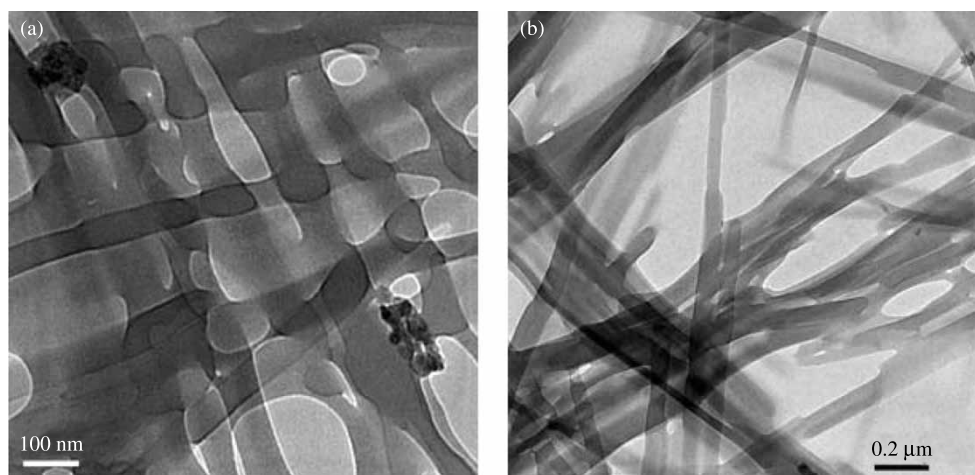


Figure 11. HRTEM images (a) and (b) of the dried gel derived from peptide **I** in toluene showing the formation of a nanofibrous network.

N-terminal protection and the C-terminus was protected as a methyl ester. N-terminal deprotection was performed using $\text{CF}_3\text{CO}_2\text{H}$. Couplings were mediated by dicyclohexylcarbodiimide (DCC)/1-hydroxybenzotriazole (HOBt). All intermediates were characterised by thin layer chromatography on silica gel and used without further purification. The final peptides were purified by column chromatography using silica gel (100–200 mesh) as the stationary phase and ethyl acetate–petroleum ether mixture as the eluent. Peptides **I** and **II** were characterised by NMR and IR.

Boc-Gly-m-ABA-OMe (I). Peptide **I** was prepared following the reported procedure (53).

Boc-Phe-Gly-m-ABA-OMe (I). To compound **1** (1.50 g, 4.87 mmol), trifluoroacetic acid (3 ml) was added at 0°C and stirred at room temperature. The removal of the Boc group was monitored by TLC. After 3 h, trifluoroacetic acid was removed under reduced pressure to afford the crude trifluoroacetate salt. The residue was taken up

in water and washed with diethyl ether. The pH of the aqueous solution was adjusted to 8 with sodium bicarbonate and extracted with ethyl acetate. The extracts were pooled, washed with saturated brine, dried over sodium sulphate and concentrated to a highly viscous liquid that gave a positive ninhydrin test. This dipeptide free base was added to a well ice-cooled solution of Boc-Phe-OH (1.29 g, 4.87 mmol) in DMF (6 ml) followed by DCC (1.50 g, 7.30 mmol) and HOBt (0.66 g, 4.87 mmol). The reaction mixture was stirred at room temperature for 3 days. The residue was taken up in ethyl acetate and DCU was filtered off, and, to the filtrate, 20 ml of ethyl acetate was added. The organic layer was washed with 2 M HCl (3×50 ml), 1 M Na_2CO_3 solution (3×50 ml) and brine, dried over anhydrous Na_2SO_4 and evaporated *in vacuo*, to yield a white solid. Purification was done using silica gel as the stationary phase and ethyl acetate–petroleum ether mixture as the eluent. Yield: 1.8 g (81.1%). Mp = $141\text{--}143^\circ\text{C}$; Elemental analysis calcd for $\text{C}_{24}\text{H}_{29}\text{N}_3\text{O}_6$ (455.51): C, 63.28; H, 6.42; N, 9.22%; Found: C, 63.18; H, 6.33; N, 9.15%. IR (KBr): 3340, 2928,

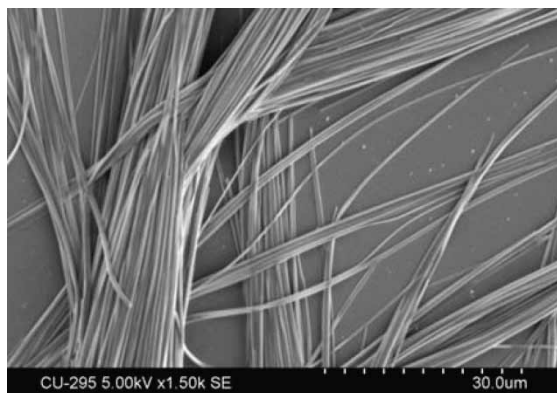


Figure 12. FE-SEM image of the fibrils of peptide **II** generated from toluene with an average diameter of 400–500 nm.

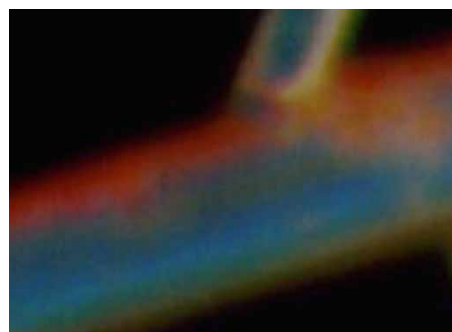


Figure 13. A dried gel of peptide **I**–toluene observed between crossed polarisers after binding with Congo red shows a bluish-green birefringence.

1695, 1654, 1527 cm^{-1} . ^1H NMR 300 MHz (CDCl_3 , δ ppm): 9.11 (*m*-ABA-NH, 1H, s), 8.21 [Ha (*m*-ABA), 1H, s], 7.96 [Hd (*m*-ABA), 1H, d, $J = 7.8$ Hz], 7.74 [Hb (*m*-ABA), 1H, d, $J = 7.8$ Hz], 7.41 [Hc (*m*-ABA), 1H, t, $J = 8.1$ Hz], 7.21–7.30 (phenyl ring protons), 7.01 (Gly-NH, 1H, t), 5.25 (Phe-NH, 1H, d, $J = 7.6$ Hz), 4.45 (C^αHs of Phe, 1H, m), 4.25–4.02 (C^αHs of Gly, 2H, m), 3.90 ($-\text{OCH}_3$, 3H, s), 3.25–3.01 (C^βHs of Phe, 2H, m), 1.44 (CH_3s Boc, 9H, s); ^{13}C NMR 75 MHz (CDCl_3 , δ ppm): 171.84, 167.26, 166.12, 155.35, 138.00, 136.50, 130.00, 128.72, 128.27, 127.91, 126.19, 124.37, 123.91, 120.34, 79.34, 55.77, 51.52, 43.08, 37.26, 27.72; HR-MS (M^+Na^+) = 478.19, M_{calcd} = 455.51.

Boc-Leu-Gly-*m*-ABA-OMe (II). To compound **1** (1.50 g, 4.87 mmol), trifluoroacetic acid (3 ml) was added at 0°C and stirred at room temperature. The removal of the Boc group was monitored by TLC. After 3 h, trifluoroacetic acid was removed under reduced pressure to afford the crude trifluoroacetate salt. The residue was taken up in water and washed with diethyl ether. The pH of the aqueous solution was adjusted to 8 with sodium bicarbonate and extracted with ethyl acetate. The extracts were pooled, washed with saturated brine, dried over sodium sulphate and concentrated to a highly viscous liquid that gave a positive ninhydrin test. This dipeptide free base was added to a well ice-cooled solution of Boc-Leu-OH (1.12 g, 4.87 mmol) in DMF (6 ml) followed by DCC (1.50 g, 7.30 mmol) and HOBt (0.66 g, 4.87 mmol). The reaction mixture was stirred at room temperature for 3 days. The residue was taken up in ethyl acetate and DCU was filtered off, and, to the filtrate, 20 ml of ethyl acetate was added. The organic layer was washed with 2 M HCl (3×50 ml), 1 M Na_2CO_3 solution (3×50 ml) and brine, dried over anhydrous Na_2SO_4 and evaporated *in vacuo*, to yield a white solid. Purification was done using silica gel as the stationary phase and ethyl acetate–petroleum ether mixture as the eluent. Yield: 1.7 g (82.9%). Mp = 118–120 $^\circ\text{C}$; Elemental analysis calcd for $\text{C}_{21}\text{H}_{31}\text{N}_3\text{O}_6$ (421.49): C, 59.84; H, 7.41; N, 9.97%; Found: C, 59.76; H, 7.34; N, 9.88%. IR (KBr): 3342, 2960, 1672, 1526 cm^{-1} . ^1H NMR 300 MHz (CDCl_3 , δ ppm): 9.15 (*m*-ABA-NH, 1H, s), 8.23 [Ha (*m*-ABA), 1H, s], 7.86 [Hd (*m*-ABA), 1H, d, $J = 7.8$ Hz], 7.72 [Hb (*m*-ABA), 1H, d, $J = 7.8$ Hz], 7.45 [Hc (*m*-ABA), 1H, t, $J = 8.1$ Hz], 7.11 (Gly-NH, 1H, t), 5.39 (Leu-NH, 1H, d, $J = 7.6$ Hz), 4.25–4.02 (C^αHs of Gly and Leu, 3H, m), 3.89 ($-\text{OCH}_3$, 3H, s), 1.62–1.82 (C^βHs and C^γHs of Leu, 3H, m), 1.43 (CH_3s Boc, 9H, s), 0.95–0.85 (C^δHs of Leu, 6H, m); ^{13}C NMR 75 MHz (CDCl_3 , δ ppm): 173.23, 167.52, 166.25, 155.74, 138.05, 130.11, 128.35, 124.51, 124.06, 120.47, 79.44, 53.41, 51.60, 43.15, 40.79, 27.84, 24.27, 22.52, 21.41; HR-MS (M^+Na^+) = 444.00, M_{calcd} = 421.49.

NMR experiments

All ^1H and ^{13}C NMR spectra of peptides **I** and **II** were recorded on a Bruker Avance 300 model spectrometer operating at 300 and 75 MHz, respectively. The peptide concentrations were 10 mM in CDCl_3 for ^1H NMR and 40 mM in CDCl_3 for ^{13}C NMR.

CD spectroscopy

Solutions of peptides **I** and **II** in methanol (1.5 mM as the final concentration) were used for obtaining the spectra. Far-UV CD measurements were recorded at 25°C with a 0.5 s averaging time and a scan speed of 50 nm/min, using a JASCO spectropolarimeter (J 720 model) equipped with a 0.1 cm path length cuvette. The measurements were taken at 0.2 nm wavelength intervals and 2.0 nm spectral bandwidth, and five sequential scans were recorded for each sample.

FE-SEM study

The morphologies of the dry gel of peptide **I** and the fibrous materials of peptide **II** generated from toluene were investigated using FE-SEM. For the FE-SEM study, the fibrous materials of the peptides were platinum coated. The micrographs were taken in a FE-SEM apparatus (JEOL JSM-6700F).

HRTEM

The morphology of the dried gel of peptide **I** generated from toluene was investigated using HRTEM. A solution of peptide **I** in toluene (1.12% w/v) was incubated overnight at room temperature. Transmission electron microscopy (TEM) studies of the peptide were done using a small amount of the solution of the peptide on carbon-coated copper grid (300 mesh) by slow evaporation and allowed to dry in vacuum at room temperature for 1 day. Images were taken by JEOL JEM-2100.

Congo red binding assay

The dried gel of peptide **I** generated from toluene was stained by the addition of alkaline Congo red solution (80% methanol/20% glass-distilled water containing 10 μl of 1% NaOH) for 2 min and then excess stain was removed by rinsing the stained gel material with glass-distilled water for several times. The stained gel was dried under vacuum at room temperature for 24 h, then visualised at $40\times$ magnification and a birefringence was observed between crossed polarisers.

WAXS

The WAXS pattern was made on the tripeptide gel of 4.0% (w/v) peptide **I** in toluene. The experiment was carried out

in a PW3040/X0 X'pert PRO diffractometer. The instrument was operated at a 45 kV voltage and 30 mA current. The sample was scanned from 2° to 55° 2θ at the step scan mode (step size 0.0170°).

Acknowledgements

A.D. would like to thank CSIR, New Delhi, India, for a senior research fellowship (SRF). The financial assistance of UGC, New Delhi is acknowledged [Major Research Project, No. 32-190/2006(SR)]. We acknowledge the financial assistance of Centre for Research in Nanoscience and Nanotechnology, University of Calcutta.

References

- Xing, B.G.; Yu, C.W.; Chow, K.H.; Ho, P.L.; Fu, D.G.; Xu, B. *J. Am. Chem. Soc.* **2002**, *124*, 14846–14847.
- Yang, Z.; Liang, G.; Guo, Z.; Xu, B. *Angew. Chem. Int. Ed.* **2007**, *46*, 8216–8219.
- Jung, J.H.; Nakashima, K.; Shinkai, S. *Nano Lett.* **2001**, *1*, 145–148.
- Ray, S.; Das, A.K.; Banerjee, A. *Chem. Commun.* **2006**, 2816–2818.
- Kiyonaka, S.; Sugiyasu, K.; Shinkai, S.; Hamachi, I. *J. Am. Chem. Soc.* **2002**, *124*, 10954–10955.
- Bhattacharjya, S.; Krishnan-Ghosh, Y. *Chem. Commun.* **2001**, 183–186.
- Kim, J.; Altreuter, D.H.; Clark, D.S.; Dordick, J.S. *J. Am. Oil Chem. Soc.* **1998**, *75*, 1109–1113.
- Murdam, S.; Gregorids, G.; Florence, A.T. *Eur. J. Pharm. Sci.* **1999**, *8*, 177–186.
- Sugiyasu, K.; Fujita, N.; Shinkai, S. *Angew. Chem. Int. Ed.* **2004**, *43*, 1229–1233.
- Ajayaghosh, A.; George, S.J.; Praveen, V.K. *Angew. Chem. Int. Ed.* **2003**, *42*, 332–335.
- Wilder, E.A.; Wilson, K.S.; Quinn, J.B.; Skrtic, D.; Antonucci, J.M. *Chem. Mater.* **2005**, *17*, 2946–2952.
- Kubo, W.; Kitamura, T.; Hanabusa, K.; Wada, Y.; Yanagida, S. *Chem. Commun.* **2002**, 374–375.
- Jung, J.H.; Kobayashi, H.; Masuda, M.; Shimizu, T.; Shinkai, S. *J. Am. Chem. Soc.* **2001**, *123*, 8785–8789.
- Kanie, K.; Sugimoto, T. *Chem. Commun.* **2004**, 1584–1585.
- Love, C.S.; Chechik, V.; Smith, D.K.; Wilson, K.; Ashworth, I.; Brennan, C. *Chem. Commun.* **2005**, 1971–1973.
- Coates, I.A.; Hirst, A.R.; Smith, D.K. *J. Org. Chem.* **2007**, *72*, 3937–3940.
- De Loops, M.; van Esch, J.; Kellogg, R.M.; Feringa, B.L. *Angew. Chem. Int. Ed.* **2001**, *40*, 613–616.
- Moniruzzaman, M.; Sundararajan, P.R. *Langmuir* **2005**, *21*, 3802–3807.
- Yoza, K.; Ono, Y.; Yoshihara, K.; Akao, T.; Shinmori, H.; Takeuchi, M.; Shinkai, S.; Reinhoudt, D.N. *Chem. Commun.* **1998**, 907–908.
- Smith, A.M.; Williams, R.J.; Tang, C.; Coppo, P.; Collins, R.F.; Turner, M.L.; Saiani, A.; Ulijn, R.V. *Adv. Mater.* **2008**, *20*, 37–41.
- Smith, A.M.; Ulijn, R.V. *Chem. Soc. Rev.* **2008**, *37*, 664–675.
- Chow, H.-F.; Zhang, J.; Lo, C.-M.; Cheung, S.-Y.; Wong, K.-W. *Tetrahedron* **2007**, *63*, 363–373.
- Xing, B.; Choi, M.-F.; Xu, B. *Chem. Commun.* **2002**, 362–363.
- Ziessel, R.; Pickaert, G.; Camerel, F.; Donnio, B.; Guillon, D.; Cesario, M.; Prangé, T. *J. Am. Chem. Soc.* **2004**, *126*, 12403–12413.
- Sugiyasu, K.; Numata, M.; Fujita, N.; Park, S.M.; Yun, Y.J.; Kim, B.H.; Shinkai, S. *Chem. Commun.* **2004**, 1996–1997.
- George, M.; Snyder, S.L.; Terech, P.; Glinka, C.J.; Weiss, R.G. *J. Am. Chem. Soc.* **2003**, *125*, 10275–10283.
- Abdallah, D.J.; Lu, L.; Weiss, R.G. *Chem. Mater.* **1999**, *11*, 2907–2911.
- Fuhrhop, J.H.; Schneider, P.; Rosenberg, J.; Boekema, E. *J. Am. Chem. Soc.* **1987**, *109*, 3387–3390.
- Koenig, J.; Boettcher, C.; Winkler, H.; Zeitler, E.; Talmon, Y.; Fuhrhop, J.H. *J. Am. Chem. Soc.* **1993**, *115*, 693–700.
- Boettcher, C.; Schade, B.; Fuhrhop, J.H. *Langmuir* **2001**, *17*, 873–877.
- Imae, T.; Takahashi, Y.; Muramatsu, H. *J. Am. Chem. Soc.* **1992**, *114*, 3414–3419.
- Pang, S.F.; Zhu, D.B. *Chem. Phys. Lett.* **2002**, *358*, 479–483.
- Suzuki, M.; Yumoto, M.; Kimura, M.; Shirai, H.; Hanabusa, K. *Chem.-Eur. J.* **2003**, *9*, 348–354.
- Banerjee, A.; Palui, G.; Banerjee, A. *Soft Matter* **2008**, *4*, 1430–1437.
- Jayakumar, R.; Murugesan, M.; Asokan, C.; Scibioh, M.A. *Langmuir* **2000**, *16*, 1489–1496.
- Ganesh, S.; Prakash, S.; Jayakumar, R. *Biopolymers* **2003**, *70*, 346–354.
- Malik, S.; Maji, S.K.; Banerjee, A.; Nandi, A.K. *J. Chem. Soc., Perkin Trans. 2* **2002**, 1177–1186.
- Maji, S.K.; Malik, S.; Drew, M.G.B.; Banerjee, A. *Tetrahedron Lett.* **2003**, *44*, 4103–4107.
- Das, A.K.; Bose, P.P.; Drew, M.G.B.; Banerjee, A. *Tetrahedron* **2007**, *63*, 7432–7442.
- Dutt, A.; Drew, M.G.B.; Pramanik, A. *Org. Biomol. Chem.* **2005**, *3*, 2250–2254.
- Gazit, E. *FASEB J.* **2002**, *16*, 77–83.
- Murata, K.; Aoki, M.; Suzuki, T.; Harada, T.; Kawabata, H.; Komori, T.; Ohseto, F.; Ueda, K.; Shinkai, S. *J. Am. Chem. Soc.* **1994**, *116*, 6664–6676.
- Karle, I.L.; Banerjee, A.; Bhattacharya, S.; Balaram, P. *Biopolymers* **1996**, *38*, 515–526.
- Makin, O.S.; Serpell, L.C. *J. Mol. Biol.* **2004**, *335*, 1279–1288.
- Bond, J.P.; Deverin, S.P.; Inouye, H.; el-Agnaf, O.M.; Teeter, M.M.; Krischner, D.A. *J. Struc. Biol.* **2003**, *141*, 156–170.
- Sundae, M.; Serpell, L.C.; Bartlam, M.; Fraser, P.E.; Pepys, M.B.; Blake, C.C.F. *J. Mol. Biol.* **1997**, *273*, 729–739.
- Sundae, M.; Blake, C. *Adv. Protein Chem.* **1997**, *50*, 123–159.
- Damas, A.M.; Saraiva, M.J. *J. Struc. Biol.* **2000**, *130*, 290–299.
- Moretto, V.; Crisma, M.; Bonora, G.M.; Toniolo, C.; Balaram, H.; Balaram, P. *Macromolecules* **1989**, *22*, 2939–2944.
- De Jong, J.; Lucas, J.D.L.N.R.; Kellogg, M.; van Esch, J.H.; Feringa, B.L. *Science* **2004**, *304*, 278–281.
- Ray, S.; Drew, M.G.B.; Das, A.K.; Banerjee, A. *Supramol. Chem.* **2006**, *18*, 455–464.
- Bodanszky, M.; Bodanszky, A. *The Practice of Peptide Synthesis*; Springer-Verlag: New York, NY, 1984; pp 1–282.
- Dutta, A.; Kar, S.; Fröhlich, R.; Koley, P.; Pramanik, A. *ARKIVOC* **2009**, *ii*, 31–43.